A General Method to Construct Single-Atom Catalysts Supported on

N-doped Graphene for Energy Applications

Linghui Liu,[ab] Song Liu,[bc] Lu Li,[b] Haifeng Qi,[bc] Hongbin Yang,[d] Yanqiang Huang,[b] Zidong Wei,[a] Li Li,[a*]

Jinming Xu,[b*] Bin Liu,[d*]

[a]School of Chemistry and Chemical Engineering, Chongqing University, Shapingba 174, Chongqing

400044, P. R. China. Email: liliracial@cqu.edu.cn

[b]State Key Laboratory of Catalysis, Dalian Institute of Chemical Physics, Chinese Academy of Sciences,

457 Zhongshan Road, Dalian 116023, P. R. China. Email: xujm@dicp.ac.cn

[c]University of Chinese Academy of Sciences, Beijing 100049, China

[d]School of Chemical and Biomedical Engineering, Nanyang Technological University, 62 Nanyang Drive,

Singapore 637459, Singapore. Email: LiuBin@ntu.edu.sg

Experimental Section

Materials

Al(OPri)$_3$ (98%), sodium fluoride (98%), anhydrous sodium acetate (99%), magnesium acetate tetrahydrate (99%), silica (15nm), phenanthroline (99%)were purchased from Aladdin, Ni(NO$_3$)$_2$·6H$_2$O (98%), Cu(NO$_3$)$_2$·3H$_2$O (98%), Fe(NO$_3$)$_3$·9H$_2$O (98%), Co(NO$_3$)$_2$·6H$_2$O (98%), KOH (99%), were purchased from Sigma-Aldrich, all reagents were used without any further purification. Carbon paper was obtained from FuelCell.

Preparation of intercalated phenanthroline in montmorillonite (PMIM)

Montmorillonite (MMT) was prepared according to a reported method.[1] Briefly, 42 g of Al(OPri)$_3$ was added into 360 g of deionized water in a 500 mL beaker maintained at 75 °C in a water bath, followed by stirring for 0.5 h. Afterwards, the temperature was raised to 95 °C to induce evaporation of isopropanol. One hour later, deionized water was added until the total weight of the solution reached 360 g to obtain aluminum hydroxide suspension. In another plastic beaker, 500 g of deionized water, 1.05 g of sodium fluoride, 3.70 g of anhydrous sodium acetate, 9.70 g of magnesium acetate tetrahydrate and 360g aluminum hydroxide suspension were added in order under mechanical agitation. After stirring for 0.5 h, 30.5 g of silica was added and the mixture was stirred for another 3 h. Afterwards, the mixture was divided into 3 parts, each ~306 g, placed in a 450 mL Teflon-lined stainless steel reactor and incubated at 220 °C for 72 h to prepare MMT with the theoretical formula of Na$_{0.4}$(Al$_{1.6}$Mg$_{0.4}$)Si$_4$O$_{10}$(OH)$_2$. Subsequently, 40 g of MMT and 20 g of phenanthroline were added into a mixed solution composing of 500 mL of deionized water and 500 mL of ethanol and stirred for 24 h. After filtration, the powder was washed with deionized water and ethanol, and dried at 60 °C overnight to obtain intercalated phenanthroline in MMT (PMIM).

Synthesis of single-atom catalyst dispersed on N-doped graphene

In a typical procedure to synthesize single-nickel atom catalyst, 7.2 g of PMIM was dispersed in 400 mL of deionized water with 7.2 g of Ni(NO$_3$)$_2$·6H$_2$O and stirred for 24 h. Then, the reaction product was filtered, washed with deionized water and ethanol, and dried at 60 °C overnight. Subsequently, the dried powder was further dehydrated at 100 °C for 1 h, followed by pyrolyzed at 900 °C for 3 h under N$_2$ atmosphere in a tube furnace. After pyrolysis, MMT was etched successively by 10 % HF and 10 % HCl with mechanical agitation to obtain single-nickel-atom catalyst dispersed on nitrogen-doped graphene. Similarly, other single-atom catalysts including Fe, Co and Cu could be synthesized by replacing Ni(NO$_3$)$_2$·6H$_2$O with Fe(NO$_3$)$_3$·9H$_2$O, Co(NO$_3$)$_2$·6H$_2$O, Cu(NO$_3$)$_2$·3H$_2$O.

Synthesis of the catalysts without MMT

2.4 g of phenanthroline and 0.079 g of Ni(NO$_3$)$_2$·6H$_2$O was dispersed in the mixed liquor of 200 mL deionized water and 200mL ethanol and stirred for 24 h, the powder collected after rotary evaporation was pyrolyzed at 900 ºC for 3 h under N$_2$ atmosphere in a tube furnace, then the catalysts without MMT was obtained.

Characterization

X-ray diffraction (XRD) was carried out on a PANalytical X'pert diffractometer with nickel-filtered Cu Kα radiation, operated at 40 kV and 40 mA.

Scanning electron microscopy (SEM) characterization was performed on a field-emission JSM-7800F microscope under backscattered electron imaging mode with 15.0 kV accelerating voltage.

The metal content was determined by Inductively Coupled Plasma Atomic Emission Spectroscopy (ICP-AES) on an IRIS Intrepid II XSP instrument (Thermo Electron Corp.).

X-ray photoelectron spectroscopy (XPS) measurements were performed on a Thermo ESCALAB 250Xi X-ray photoelectron spectrometer with a monochromatized X-ray source (Al Kα = 1846.6 eV), operated at 15 kV and 10.8 mA.

Transmission electron microscopy (TEM) characterization was conducted on JEOL JEM-2100F at 200 kV. The high-angle annular dark field scanning transmission electron microscope (HAADF-STEM) measurements were

conducted on a JEOL JEM-ARM200F STEM/TEM microscope with a guaranteed resolution of 0.08 nm.

X-ray absorption spectroscopy (XAS) spectra including both X-ray absorption near-edge structure (XANES) and extended X-ray absorption fine structure (EXAFS) were collected at the BL 14W1 of Shanghai Synchrotron Radiation Facility (SSRF), Shanghai Institute of Applied Physics (SINAP), China. A double Si (111)-crystal monochromator was used for energy selection. The spectra were collected at transmission mode at room temperature. The Athena software package was used to analyze the data.

Electrochemical Measurement

Electrochemical measurements of CO_2 reduction reaction were carried out in an H-type glass cell separated by Nafion 117 membrane. A Solarton workstation was employed to record the electrochemical response. The working electrode was prepared by the following process: 10 mg ml^{-1} catalyst ink was prepared by dispersing 5 mg sample and 10 μl Nafion solution (5 wt%) in 490 μl ethanol solution, was brush-painted directly onto a dry carbon fiber paper at a temperature of 50 °C, giving a catalyst loading of 1mg cm^{-2}. While a Pt foil was applied in the three-electrode system as the counter electrode and a saturated calomel electrode (SCE) as the reference electrode. For the faradaic efficiency analysis, gas products were analyzed by an online gas chromatography (GC, Agilent 7890B). During the reaction, CO_2/ N_2 gas was bubbled into the cell at a flow rate of 20 mL/min.

The measured potentials vs. saturated calomel electrode was converted to the reversible hydrogen electrode (RHE) scale according to the Nernst equation:

$$E_{RHE} = E_{SCE} + 0.2415V + 0.0592V \times pH$$

For CO_2-saturated 0.5 M $KHCO_3$ (pH=7.3), N_2-saturated 0.5 M $KHCO_3$ (pH=8.6).

The faradaic efficiencies of the gas products were calculated by Faradic efficiency calculation based on the definition of Faradic efficiency[2]:

$$FE_i = \frac{z_i \times v_i \times G \times F \times P_0}{I \times R \times T_0 \times 60000}$$

i: CO, H_2; z_i: number of electrons required to produce an *i* molecule; G: the volumetric flow rate; F: Faradaic constant; P_0: atmospheric pressure; I: the average current in a period (t) of electrocatalysis; T_0: reaction temperature; R: ideal gas constant.

The Tafel slope was calculated by the followed equation:

$$\eta = a + b\lg i$$

All the electrochemical measurements of oxygen reduction reaction were carried out in a conventional three-electrode system on an autolab station. A rotating disk electrode (RDE) and rotating ring-disk electrode (RRDE) after loading the electrocatalyst was used as the working electrode. Ag/AgCl (3.5M KCl solution) and a graphite rod were used as reference and counter electrode, respectively. The electrochemical experiments were conducted in O_2 saturated 0.1 M KOH electrolyte for the oxygen reduction reaction. 5 mg of catalyst was dispersed in 1 ml of solution containing 0.495 ml of isopropanol and 0.495 ml of water and 10 μl of 0.5 wt% Nafion solution and then sonicated for 1h to form a homogeneous catalyst ink. Then a certain volume of the catalyst ink was pipetted onto the GC surface with the nonprecious catalyst loading was 0.5 mg cm^{-2} and the loading of Pt/C was 0.102 mg cm^{-2}. Before tests, Ar/O_2 flow was carried out through the electrolyte in the cell for about 30 min to achieve the Ar/O_2-saturated solution. The cyclic voltammetry (CV) tests were measured in Ar- and O_2-saturated 0.1 M KOH solution with a scan rate of 50 mV s^{-1}. The linear sweep voltammograms (LSVs) on RDE tests were conducted with a sweep rate of 10 mV s^{-1} at room temperate. Furthermore, the stability of Fe-SAC and Pt/C was measured in O_2-saturated 0.1 M KOH solution at 0.464V vs. RHE with loading 0.5 mg cm^{-2} and 0.25mg cm^{-2}, respectively.

The measured potentials vs. Ag/AgCl electrode was converted to the reversible operated in O_2-saturated 0.1 M KOH solution hydrogen electrode (RHE) scale according to the Nernst equation:

$$E_{RHE} = E_{SCE} + 0.197 + 0.0592V \times pH$$

For Ar/O_2-saturated 0.1 M KOH (pH=13).

The $HO_2^-\%$ and the electron transfer number (n) were determined by the followed equations:

$$HO_2^-\% = 200 \times \frac{I_r/N}{I_d + I_rN}$$

$$N = 4 \times \frac{I_d}{I_d + I_rN}$$

where I_d is the disk current, I_r is the ring current and N is the current collection efficiency (N is 0.37 from the reduction of $K_3Fe[CN]_6$).
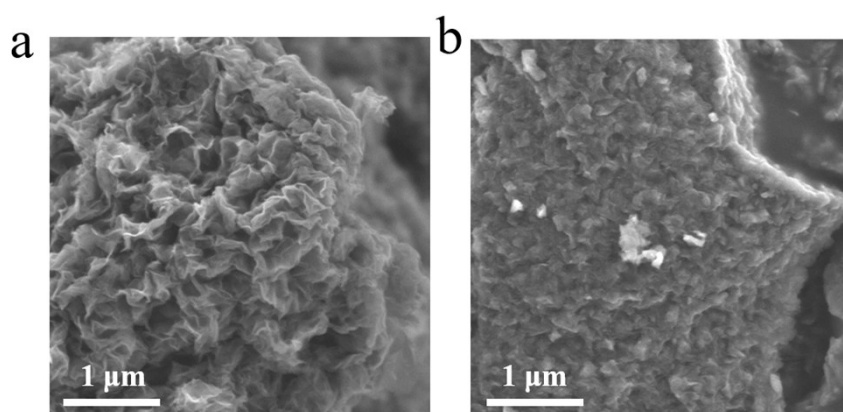
Supplementary Figures and Tables

Fig. S1 SEM images of (a) Ni-SAC and (b) The catalysts synthesis without MMT template.
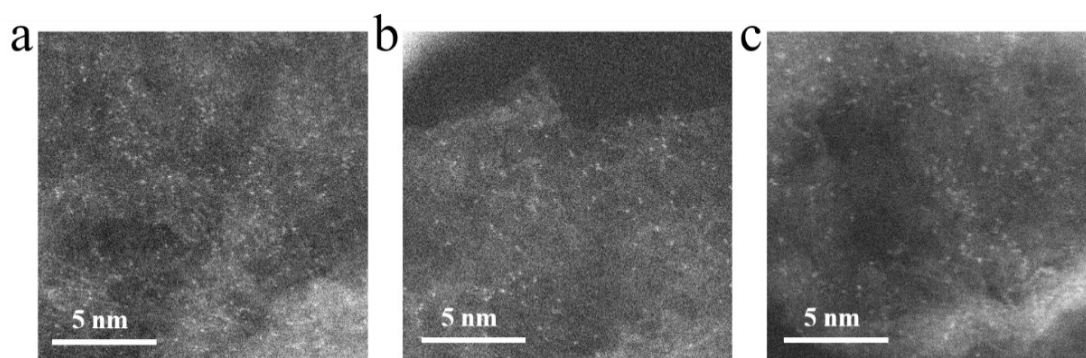
Fig. S2 HAADF-STEM images of (a) Fe-SAC, (b) Co-SAC and (c) Cu-SAC.
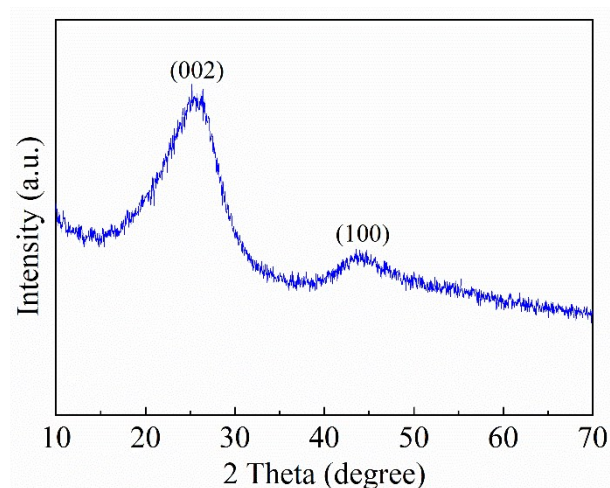
Fig. S3 XRD pattern of Ni-SAC.
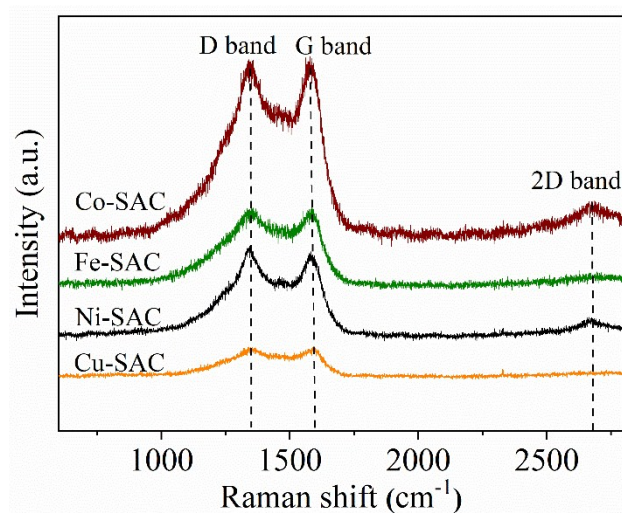
Fig. S4 Raman spectra of Ni-SAC, Fe-SAC, Co-SAC, Cu-SAC.
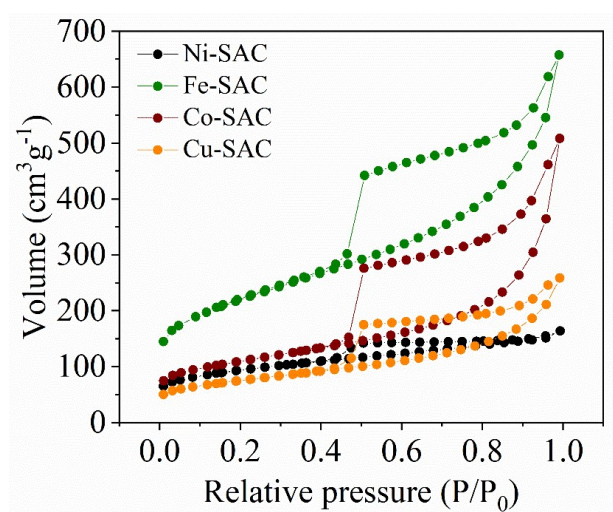
Fig. S5 N_2 adsorption–desorption isotherms of M-SACs. Ni-SAC, Fe-SAC, Co-SAC, Cu-SAC samples had large surface areas (308 m^2/g, 746 m^2/g, 374 m^2/g, 258 m^2/g), while the catalysts without template had only 1 m^2/g surface area.
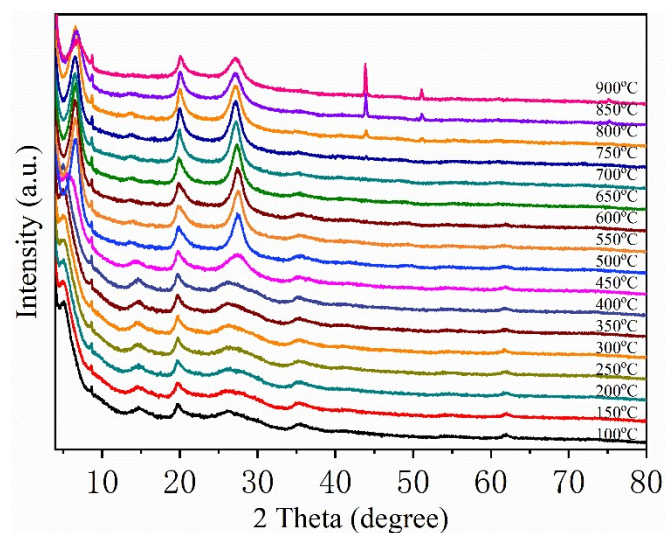
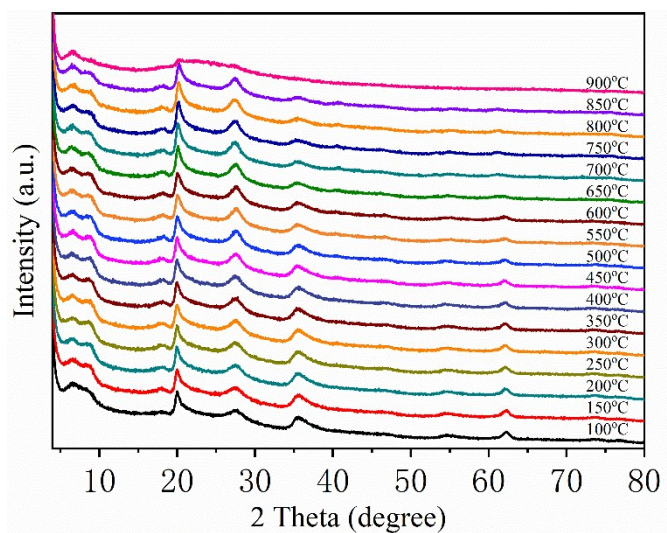**Fig. S6** In-situ XRD patterns of the carbonization process of [Ni (phen) $_n^{2+}$]-MMT.

Fig. S7 In-situ XRD patterns of the carbonization process of MMT.
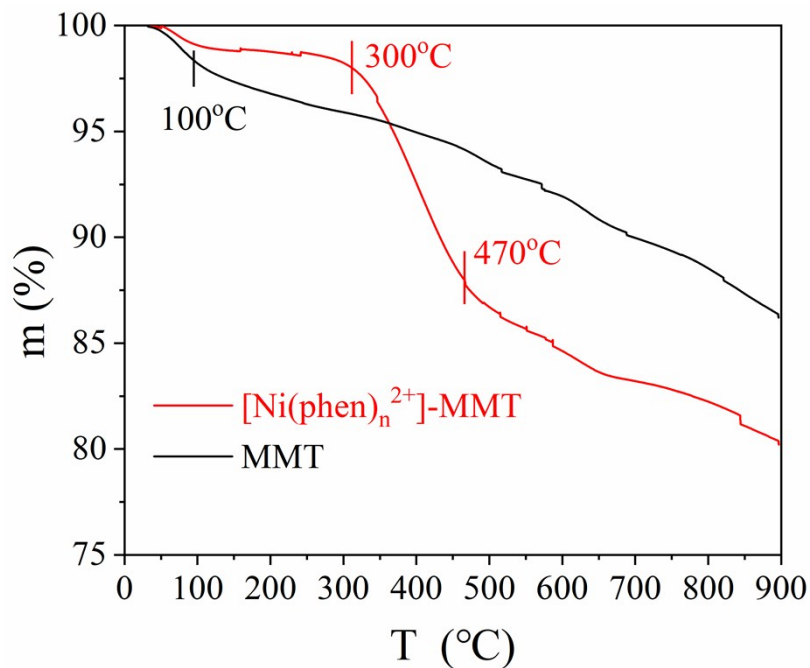
Fig. S8 TGA results of [Ni (phen)$_n^{2+}$]-MMT and MMT.
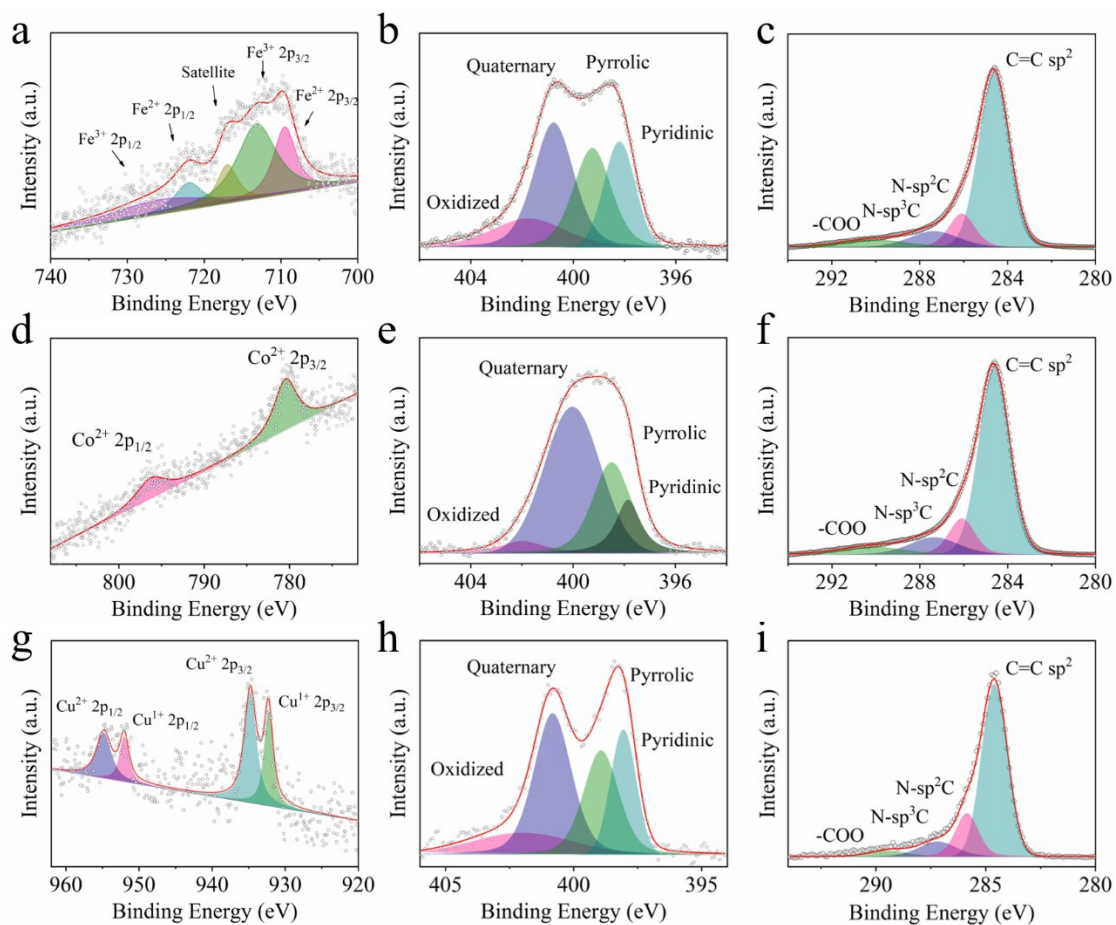
Fig. S9 Fe 2p, N 1s and C 1s XPS spectra of Fe-SAC (a, b & c). Co 2p, N 1s and C 1s XPS spectra of Co-SAC (d, e & f).

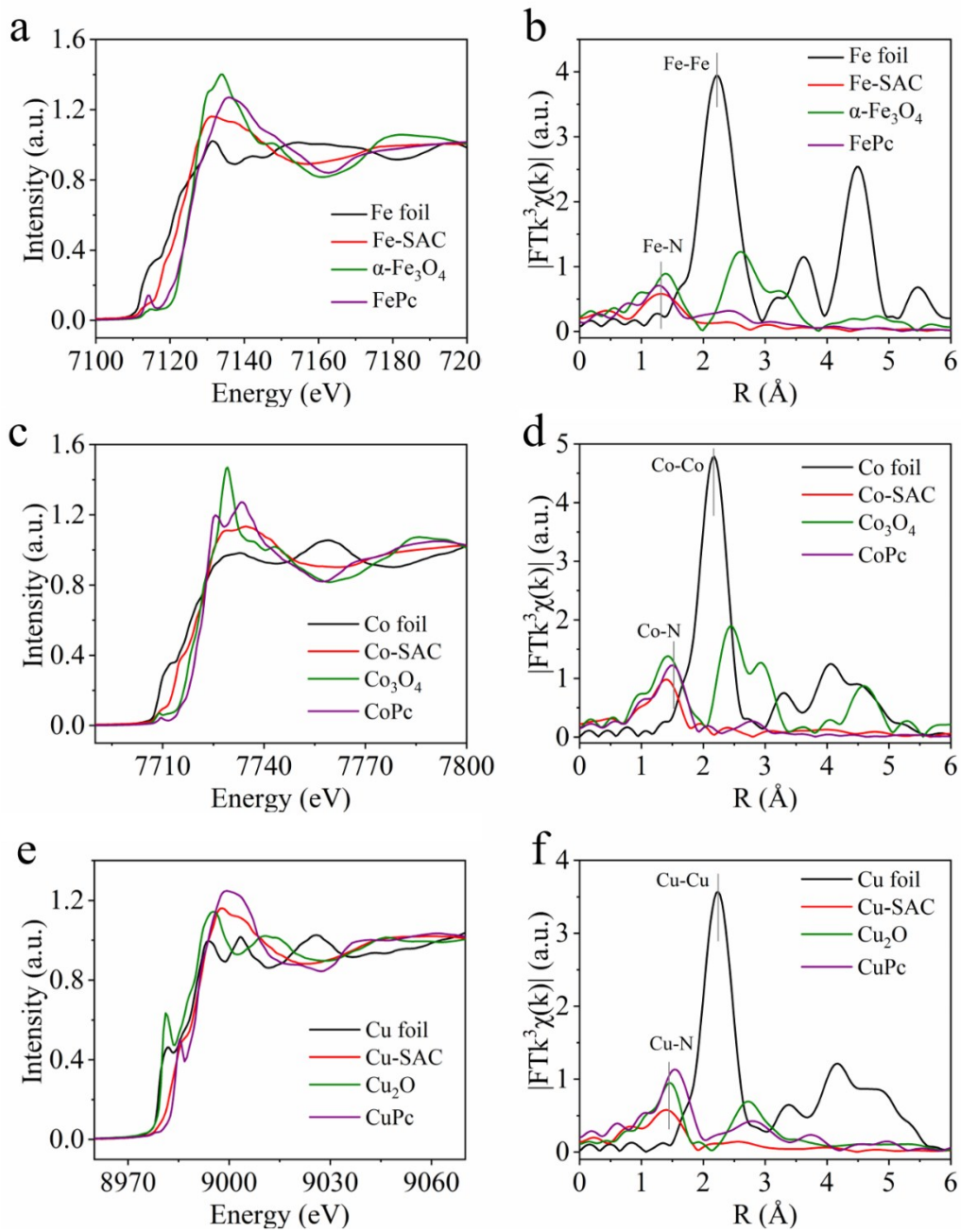Cu 2p, N 1s and C 1s XPS spectra of Cu-SAC (g, h & i).

Fig. S10 (a, c & e) Normalized XANES spectra of the Fe, Co and Cu K-edge of Fe-SAC, Co-SAC and Cu-SAC. (b, d & f)

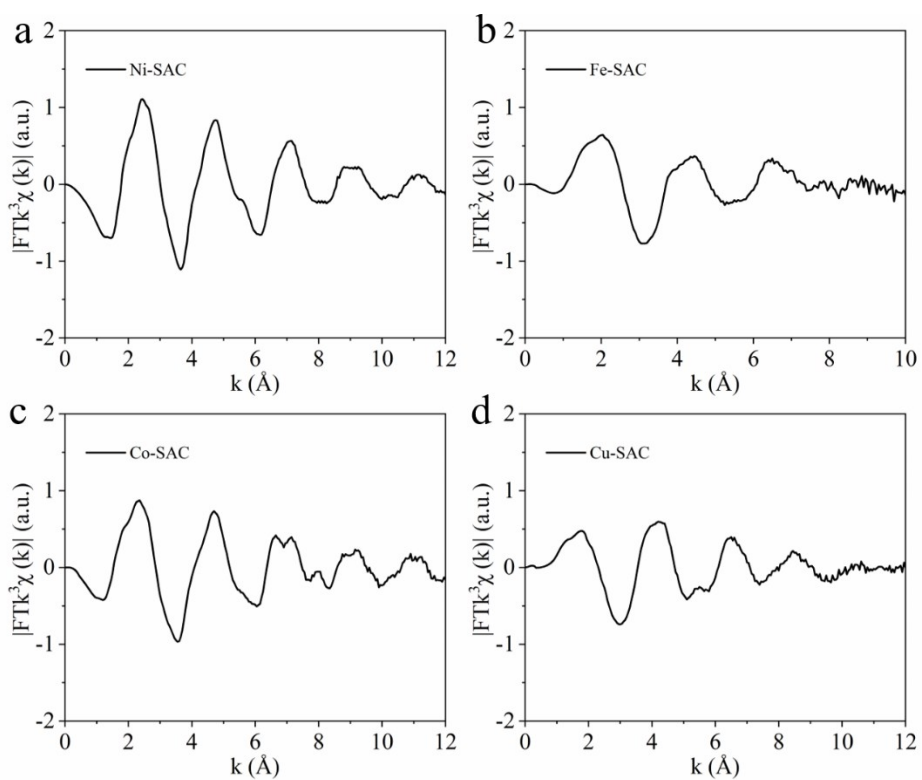The k^3-weighted Fourier transform spectra of Fe-SAC, Co-SAC and Cu-SAC.

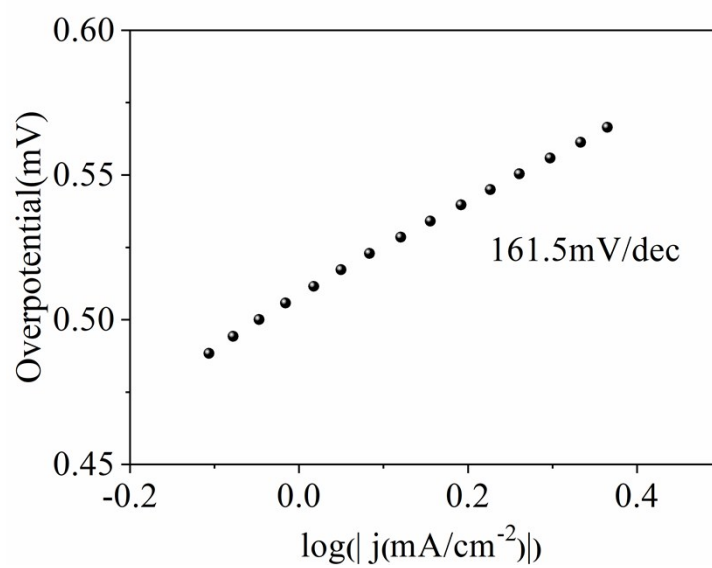**Fig. S11** EXAFS oscillation patterns of (a) Ni-SAC, (b) Fe-SAC, (c) Co-SAC, and (d) Cu-SAC.

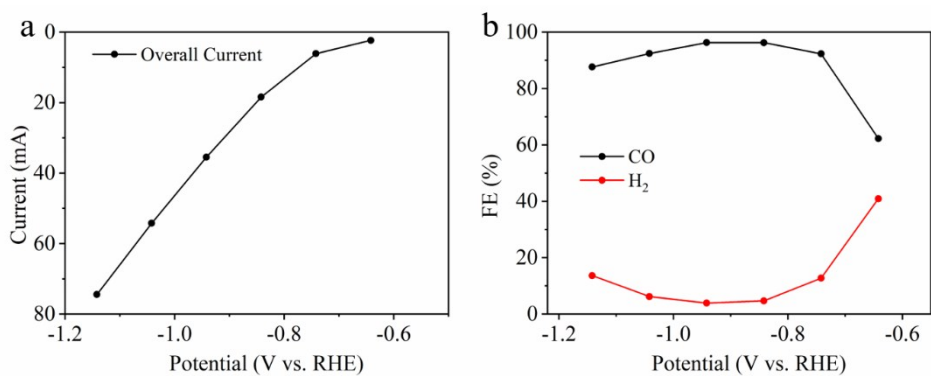

Fig. S12 Tafel slope of Ni-SAC in CO_2RR.

Fig. S13 (a)The steady-state current of Ni-SAC in a flow cell. (b) The Faradaic efficiency for CO and H$_2$ of Ni-SAC in a flow cell.
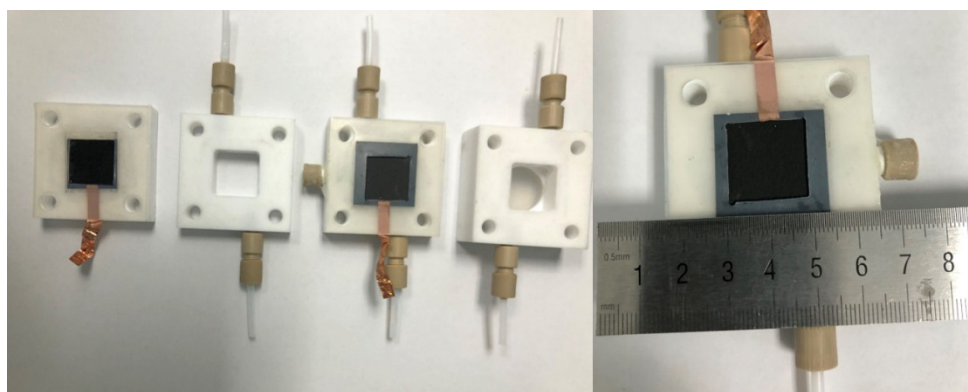

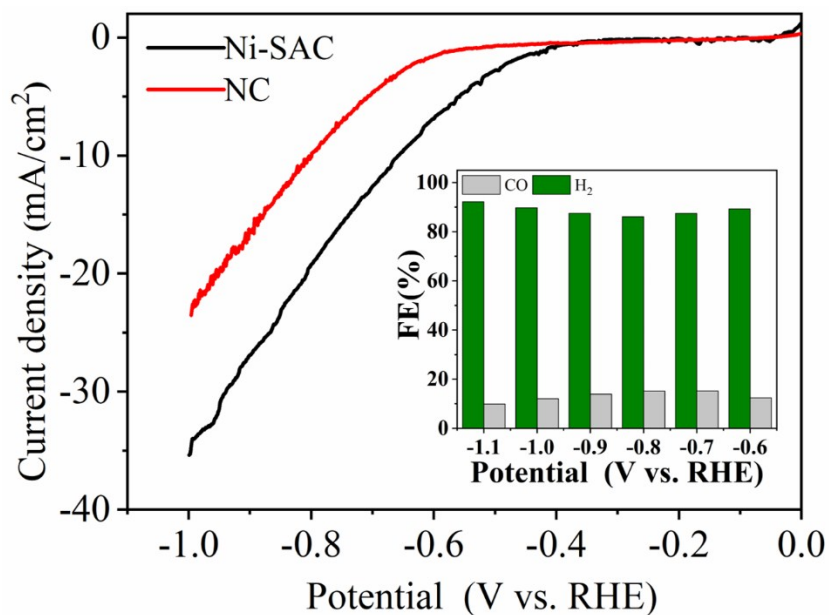**Fig. S14** Photographs of the flow cell.

Fig. S15 LSV curves of Ni-SAC (black) and NC (red) recorded in a 0.5 M KHCO$_3$ solution on carbon paper at a scan rate of 5 mV s^{-1}. Inset shows the Faradaic efficiency of NC for CO (grey bars) and H$_2$ (green bars).
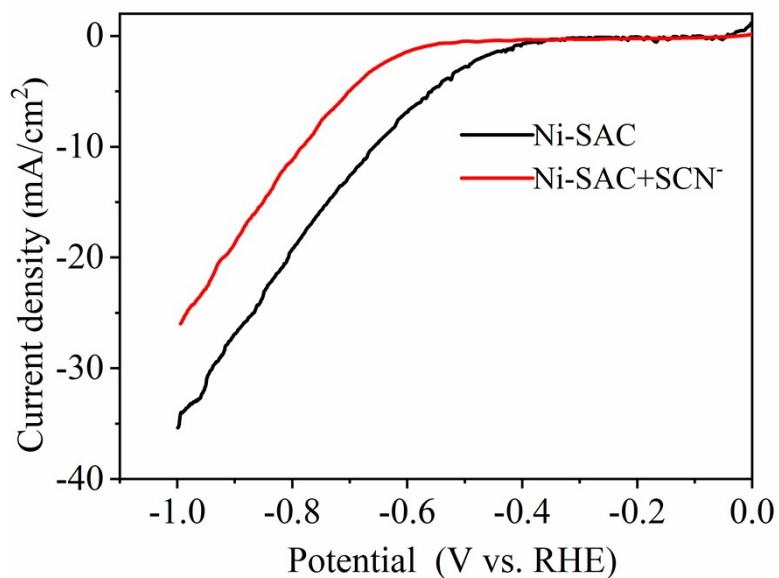
Fig. S16 LSV curves of Ni-SAC in a 0.5 M KHCO$_3$ solution with (red) and without (black) 0.02 M KSCN.
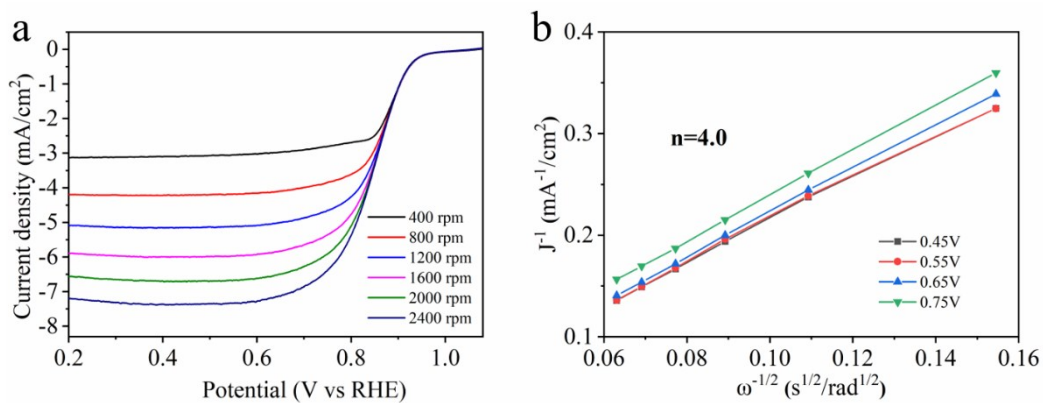

Fig. S17 (a) LSV curves of Fe-SAC with various rotation rates in O$_2$-saturated 0.1 M KOH solution. (b) The electron transfer number.
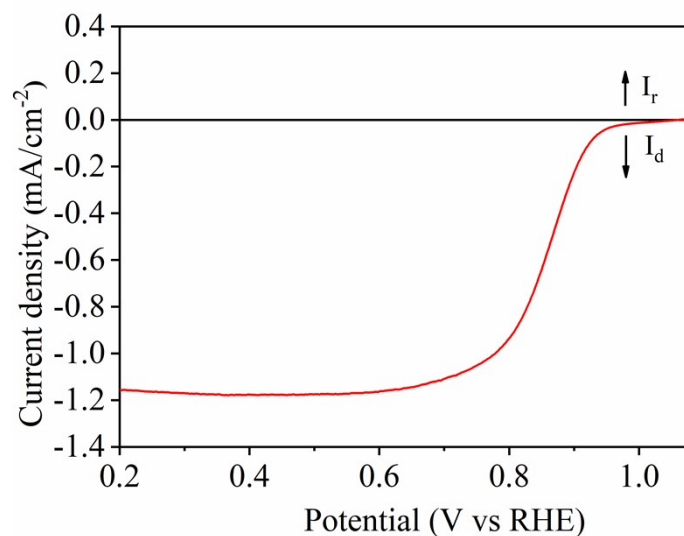

Fig. S18 RRDE curves of Fe-SAC collected at a scan rate of 5 mV s^{-1} and a rotation speed of 1600 rpm in an O$_2$-saturated 0.1 M KOH aqueous solution.

Table S1 Summary of the M content in M-SACs by ICP-AES.

Sample	Ni-SAC	Fe-SAC	Co-SAC	Cu-SAC
M (at%)	1.39	0.13	0.32	0.97

Table S2 E_0 values of the Ni-SAC and reference samples.

Sample	Ni foil	Ni-SAC	NiO	NiPc
E_0(eV)	8333.0	8338.7	8345.5	8339.2

Table S3 Ni K-edge EXAFS curve Fitting Parameters.

sample	path	N	R (Å)	σ^2 (Å^2)	ΔE_0 (eV)	R, %
Ni foil	Ni–Ni	12	2.48	0.006	7	0.002
Ni-SAC	Ni-N	4	1.85	0.005	-0.9	0.0003

N, the coordination number. R, the average absorber–backscatter distance. σ^2, the Debye–Waller factor. ΔE_0, the inner potential correction. The accuracies of the above structural parameters were estimated as N, ±20%; R, ±1%; σ2, ±20%; ΔE0, ±20%. The data range used for data fitting in k-space (Δk) and r-space (Δr) are 3.0-11.5 Å^{-1} and 1.0-1.8 Å.

Reference

1. M. Reinholdt, J. Miehe-Brendle, L. Delmotte, M. H. Tuilier, R. le Dred, R. Cortes and A. M. Flank, *Eur. J. Inorg. Chem.*, 2001, **2001**, 2831-2841.
2. H. B. Yang, S.-F. Hung, S. Liu, K. Yuan, S. Miao, L. Zhang, X. Huang, H.-Y. Wang, W. Cai, R. Chen, J. Gao, X. Yang, W. Chen, Y. Huang, H. M. Chen, C. M. Li, T. Zhang and B. Liu, *Nature Energy*, 2018, **3**, 140-147.